

Optical band gap energy and urbach tail of CdS:Pb²⁺ thin films

M. Chávez^a, H. Juárez^a, M. Pacio^a, X. Mathew^c, R. Gutiérrez^b, L. Chaltel^b, M. Zamora^b and O. Portillo^{b,*}

^aCentro de Investigación en Dispositivos Semiconductores, del Instituto de Ciencias de la Universidad Autónoma de Puebla, Av. 14 Sur Col Jardines de San Manuel, Ciudad Universitaria, Puebla, Pue., México.

^bLab. Mat. Sci. Facultad de Ciencias Químicas, Universidad Autónoma de Puebla. Puebla, Pue., P.O. Box 1067, 72001 México.

*Tel. (01 222) 2-29-55-00 Ext. 7519.

e-mail: osporti@yahoo.mx

^cInstituto de Energía Renovables, Universidad Nacional Autónoma de México, Temixco, Morelos, Mexico.

Received 14 May 2015; accepted 27 November 2015

PbS-doped CdS nanomaterials were successfully synthesized using chemical bath. Transmittance measurements were used to estimate the optical band gap energy. Tailing in the band gap was observed and found to obey Urbach rule. The diffraction X-ray (XRD) show that the size of crystallites is in the ~33 nm to 12 nm range. The peaks belonging to primary phase are identified at $2\theta = 26.5^\circ$ and $2\theta = 26.00^\circ$ corresponding to CdS and PbS respectively. Thus, a shift in maximum intensity peak from $2\theta = 26.4^\circ$ to 28.2° is clear indication of possible transformation of cubic to hexagonal phase. Also peaks at $2\theta = 13.57^\circ$, 15.9° correspond to lead perchlorate thiourea. The effects on films thickness and substrate doping on the band gap energy and the width on tail were investigated. Increasing doping give rise to a shift in optical absorption edge ~0.4 eV

Keywords: Cadmium sulfide; thin films; solar cells; optical band gap; urbach tail.

PACS: 81.10.Bk; 81.05.Dz; 81.10.-h; 81.10.Dn; 81.15.-z; 81.15.Rs

1. Introduction

There is great interest in materials science and engineering of semiconducting quantum dots, deposited as thin solid films. Such increased interest in these materials is due to the effect of quantum confinement as a partner with decreasing grain size. As the nanodimensions of semiconducting crystals affect significantly the band structures of these materials, therefore essentially all of their properties are influenced by the crystal size reduction. It is exactly this point that allows to design a semiconducting material with predefined optical and structural properties by simply controlling the crystal size. For example, the band gap energy (E_g) and structural properties of various semiconducting materials can nowadays be tuned rather precisely by an appropriate choice of the synthetic route. In general, the thin films of semiconducting quantum dots have potential applications in solar cells, light-emitting diodes, batteries, etc. One of the most important material parameters, which mostly determine the field of application of a given semiconductor, is its E_g value. In other words, the collection of materials-based control allows monitoring E_g the optical and structural properties of these semiconductor materials.

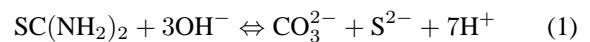
In 1953, Urbach proposed an empirical rule for the optical-absorption coefficient $\alpha(\omega)$ associated with electronic transition from the valence to conduction band tail in disordered solids. CdS thin films have been the best heterojunction partner for CdTe which is an ideal absorber in thin-film solar cells [1]. On the other hand, Chemical Bath (CB) is one of the low-cost and highly-efficient routes for depositing CdS, PbS thin films [2,3]. It have been reported that the

band gap energy (E_g) for as-deposited films decreases with increasing Cd/S [4]. Most studies have examined the optical properties of CdS thin films, but few have studied

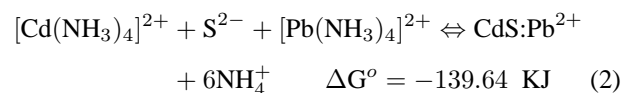
the relations between E_g and films thickness and the tailing in the E_g [5]. In this work, the thickness dependence of the E_g and Urbach tail for Pb-doped cadmium sulfide (CdS:Pb) thin films prepared by CB is reported.

2. Chemical reactions

Considering a general chemical bath reaction, thiourea hydrolysis $\text{SC}(\text{NH}_2)_2$ leads to the formation of S^{2-} and CO_3^{2-} ions according to [6]



In general form for doped samples:

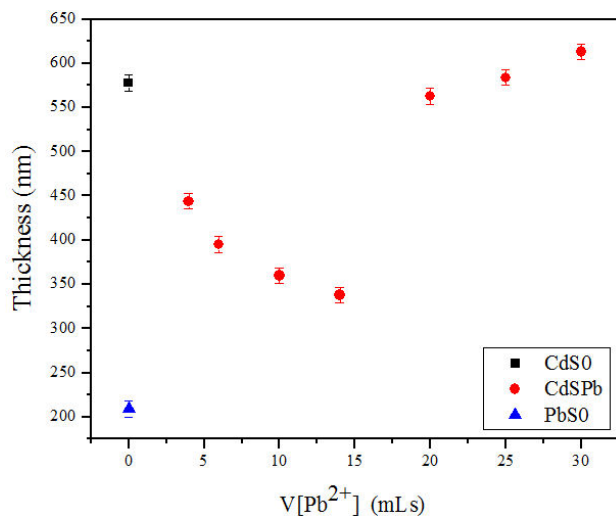


According with these results, $\Delta G^\circ > 0$, the reaction (2) is spontaneous.

Preparation of polycrystalline thin films on glass substrates was performed at a temperature of $90 \pm 2^\circ\text{C}$, both undoped and doped CdS films with seven different levels of doping ($V_{[\text{Pb}^{2+}]}$) were obtained by the addition in situ of: 4, 6, 8, 10, 14, 20, 25, 30 mLs in the solutions for CdS0 growth respectively: CdCl_2 (0.02 M), KOH (0.1 M), NH_4NO_3 (1.2 M), $\text{SC}(\text{NH}_2)_2$ (0.1 M), the doping solution $\text{Pb}(\text{CH}_3\text{CO}_3)_2$ ($V_{[\text{Pb}^{2+}]}$) 0.02 M. The samples were labelled as PbS0-CdS0



FIGURE 1. Photography of CdS0-CdSPb-PbS0 thin films.

FIGURE 2. Thickness vs. $V_{[Pb^{2+}]}$ CdS0-CdSPb-PbS0 thin films

for the undoped and CdSPb4,...,CdSPb30 for the doped samples.

The optical absorption studies were carried out using a UV-VIS-IR spectrophotometer (Cary-5000). The thickness was determined by utilizing a Veeco (Bruker), DEKTAK 150 profilometer Stylus of 12 μm . Crystalline structure characterization X-ray diffraction (XRD) patterns were registered in a D8 Discover diffractometer, using the Cu $K\alpha$ line.

3. Results and discussion

Figure 1 shows the photography of CdS0-CdS:Pb-PbS0. Figure 2 shows the thicknesses vs. $V_{[Pb^{2+}]}$ of CdS0-CdS:Pb-PbS0 thin films. Measurements of thickness decrease of ~625-325 nm range for CdSPb4 to CdSPb10 as total thickness of the films growth.

Figure 3 shows the optical transmittance (T) vs. wavelength for CdS0-CdS:Pb-PbS0 samples. The T spectra showed less transparency with CdS0 film. This may be attributed to more scattering of photons by the introduction of dopant as foreign Pb²⁺ ions, which may reduce T. This decrease in T with doping is expected, because doping increases the number of the charge carriers which increases the absorption in the film, and decreases the transmission of light [7].

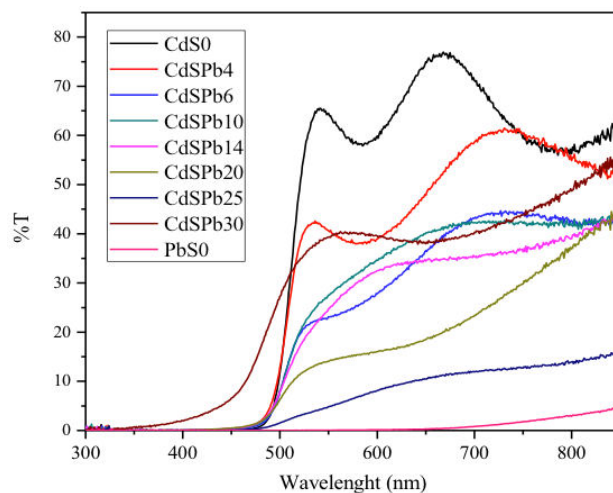
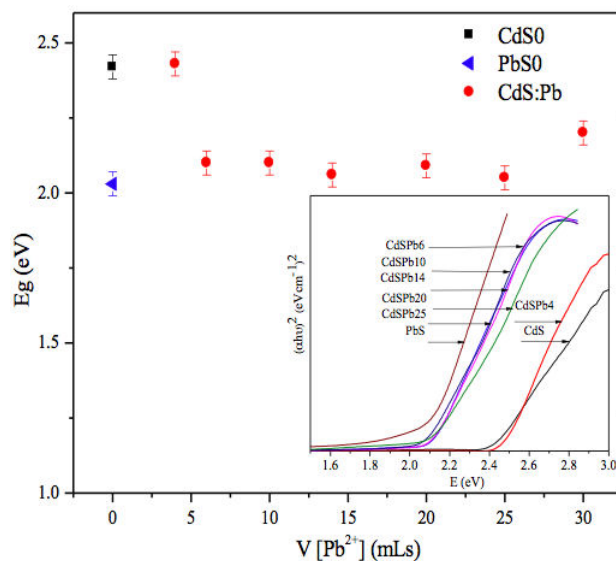


FIGURE 3. Optical transmittance spectra of the CdS, CdS:Pb, PbS thin films.

FIGURE 4. Band gap energy of the CdS0-CdSPb-PbS0 films. Inset show $(\alpha h\nu)^2$ vs photon energy.

As the Fig. 3 shows, the T of the films for wavelength values smaller than the cut-off wavelength (~ 510 nm) is a function of film thickness; that the T decreases as function of thickness and doping. The observations are in agreement with Sahay *et al.* [8]. As T decreases; however more decrement is observed in the CdSPb20 and CdSPb30 samples. It is usually presumed that the T of the films decreases with grain size in the visible region of spectrum due to light scattering on their rough surfaces. From the T spectra we have calculated the E_g of the CdSPb thin films. The absorption coefficient α and the incident photon energy $h\nu$ are related by the following equation [9]

$$\alpha h\nu = (E_g - h\nu)^n \quad (3)$$

The usual method of determining E_g is to plot a graph $(\alpha h\nu)^2$ vs. $h\nu$ and then looking for that value of n which gives best linear graph in the band edge region [9,10].

The inset in Fig. 4 shows $(\alpha h\nu)^2$ vs. $h\nu$ of the CdS0-CdS:Pb-PbS0 thin films. It can be seen that there is a difference in slope between CdSPb4 and CdSPb30 samples in the of 320-450 nm. wavelength range. This anomaly could be due to the difference in sample thickness which was ~ 200 -600 nm [11]. At any value of Pb concentration the optical E_g , this can be attributed to improvement of crystal-linity [12]. Also, during the doping, at the surface and at the grain boundaries the process would create traps within the band gap that may cause formations of the states near the band edge and so lead to a E_g shrinkage. The blue shift is also indicative of size quantization in PbS0-CdS:Pb na-noparticles. It is observed that E_g decreased within increase in doping, the reason for this fact may be attributed the decrease in thickness [13]. This means extending tail states within the E_g that leads to the E_g narrowing. The E_g vs. $V_{[Pb^{2+}]}$ values of the CdSPb are showed in Fig. 4, such values are in 2.1-2.4 eV range. As the doping content in-creases, the donor levels become degenerated and merge with the conduction band of CdS0, causing the conduction band to extend into the forbidden region which reduces the E_g [14]. However, for PbS0, $E_g = 1.94$ eV and $E_g = 3.14$ eV are related to the E0 and E1 transitions respectively [16]. These data and the literature values are used for modeling of the optical constants of PbS over 0.3-5.5 eV photon energy range, including the $E_g = 0.4$ eV region. Calculated spectra of $E_g = 2.0$ eV $(\alpha h\nu)^2$ vs. $h\nu$ are in satisfactory agreement with the experiment over the entire range of photon energies. In the low photon energy range it is as-sumed that the spectral dependence of absorption edge follows the empirical Urbach rule given by [15]

$$\alpha(\nu) = \alpha_0 \exp\left(\frac{h\nu}{E_e}\right) \quad (4)$$

Where α_0 is a constant, E_e denotes an energy which is constant or weakly dependent on temperature and is often interpreted as the width of the tail of localized states in the E_g . A plot of $\ln(\alpha)$ against the photon energy is shown in the inset in Fig 5. It was found that the optical absorption edge shifted to higher wavelengths as the films thickness and electrical resistivity diminishes for thicker films [16]. This was attributed to an increase of crystalline size, the degree of preferred orientation, internal microstrain and stoichiometry on the film [17]. The width of Urbach tail (E_e) was obtained from the fit and the results were inserted in Table I.

TABLE I. Estimated values of band gap energy and width of Urbach tail with the corresponding values of film thickness for CdS0-CdSPbS-PbS0.

Sample	thickness (nm)	E_g	E_e (meV)
CdS0	578	2.43	112.2
CdSPb4	444	2.44	80.9
CdSPb14	563	2.06	55.8
CdSPb25	584	2.09	24.6
CdSPb30	613	2.05	29.5
PbS0	209	2.2	119.6

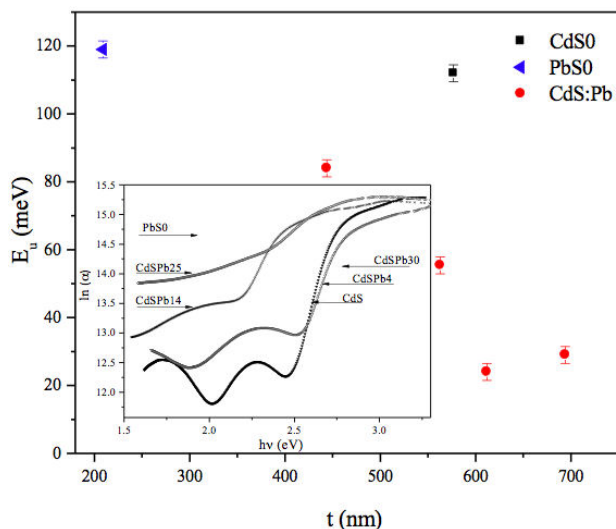


FIGURE 5. Relation between E_e and the thickness for CdS0-CdSPb-PbS.

The relation between E_e and the thickness is displayed in Fig. 5, where a decrease of width of Urbach tail with film thickness can be observed. The relation with thickness of films is not apparent because the values of film thickness are close to each other in each case. The decreases with film thickness are due to an increase of order, because as it was mentioned earlier, the crystallization is better with film thickness. These results support our interpretation of the decrease of E_g with doping as mentioned before, since the decrease of E_e with doping and thickness is an indication of the smaller density of localized states. But the films thickness in their work is also varying so, in our opinion, this decrease in E_e is not only related to the doping but also to film thickness. So the E_g value in the case of no tailing decreases with the increase of doping, in accordance with the known situation of semiconductors. This result supports our aforementioned explication of the decrease of E_g with the doping that is the doping results in films with more order and smaller density of localized states. Belgin *et al.* [5] obtained E_e values in the 122-175 eV range for ultrasonically sprayed CdS films. This linear relation between E_g and width of Urbach tail is similar to the results reported by Melsheimer *et al.* [18] and Shadia *et al.* [7].

Figure 6 shows the XRD diffraction patterns for CdS0-CdS:Pb-PbS0 samples. CdS exists in two crystalline modifications: the Wurtzite (WZ) [19] and zinc blende (ZB) phase [20]. As can be seen, the obtained diffraction pattern for CdS0 sample shows a predominant peak at $2\theta = 26.5^\circ$ which can be assigned to (111) plane of ZB CdS phase. Moreover, the intensity of peak at $2\theta = 28.2^\circ$ is due to diffraction from the (101) plane WZ phase whereas the peak at $2\theta = 26.4^\circ$ position can be co-occupied by the (111) plane of ZB phase as well as the (002) plane WZ. However, the maximum peak intensity for both phases are different, *i.e.*,

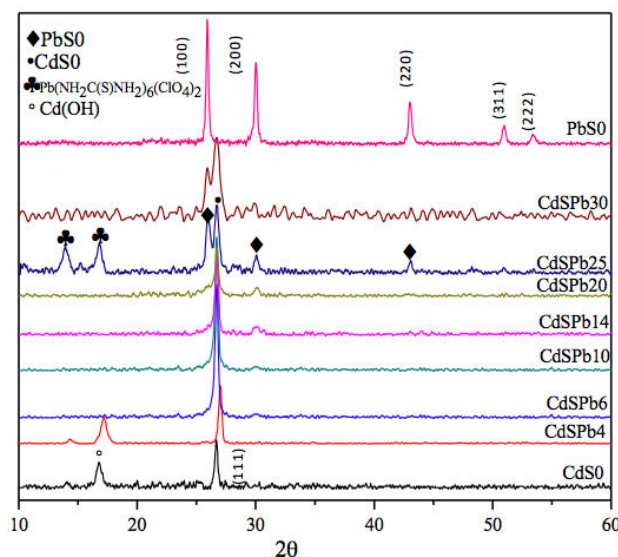
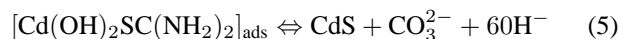


FIGURE 6. XRD diffraction patterns for CdS0-CdS:Pb-PbS0 films.

ZB maximizes at $2\theta = 26.4^\circ$ corresponding to the (111) plane, whereas WZ phase has its maximum intensity peak at $2\theta = 28.2^\circ$, corresponding to the (101) plane. However, formation of the WZ phase is likely, at least to large extent, because the characteristic diffraction peak from the (002) planes of the structure were completely absent when the CdS0 film was deposited. The shift in the diffraction angles is due to the incorporation of Pb^{2+} ion at the sublattices sites of Cd^{2+} . The diffraction peaks of CdSPb4-CdSPb10 samples and their relative intensity were affected by changing the $V_{[\text{Pb}^{2+}]}$. It is reported in the literature that at room temperature the probability that CdS dissolves in the PbS lattice is very low [21]. In this case of extremely small particles, where the contribution of surface free energy is very important, some deviations cannot be excluded. In the CdS0 and CdSPb4 samples, a cadmium hydroxide $[\text{Cd}(\text{OH})_2]$ film is clearly seen to have deposited. The formation of $\text{Cd}(\text{OH})_2$ preceding a CdS deposition can be explained by the fact that cadmium ions are labile in aqueous media and equilibria are rapidly stabilized in solution [21].

The concentration of sulfide ions is limited by the thiourea decomposition and the decomposition of the weak acid H_2S , $k_a = 9.1 \times 10^{-8}$. The activation energy for the films growth has been found as 56.7 kJ, it is close to the value for the hydrolysis of thiourea, which was used as sulfur source in CB. It was therefore supposed that the rates of both the films growth and precipitation are limited by that of the hydrolysis of thiourea in the alkaline medium. These diffraction peaks become sharper for CdSPb4, CdSPb6 and CdSPb14. From XRD patterns it can be assured that the Pb lead to PbS according to the peak located 30° in CdSPb14 to CdSPb30 samples. However, CdSPb6 sample shows a peak at $\sim 26.5^\circ$ indicating a preferred orientation. The XRD study displays that the formation of the CdS:Pb occurs in the early stage, following by the formation of PbS0 nanocrystallites in

the stage of the film growth, although the formation of films from the bath in absence of acetic is also observed [19]. It is found in this study that the reaction leads to the formation of nanocrystalline PbS0 films together with a slight decrease in the size of crystallites. These peaks do not match exactly with the reported plane spacing for ZB and W phases; it can be explained by the broadening of the peaks of CdSPb25 and CdSPb30, which can be due to small size of the crystals and by presence of strains that poses multiple facet diffraction peaks. This is the result of multidirectional growth of the synthesized nanocrystals. The peaks belonging to primary phase are identified at the $2\theta = 26.5^\circ$ and $2\theta = 26.00^\circ$ corresponding to CdS0 and PbS0 respectively. Thus, a shift in maximum intensity peak from $2\theta = 28.2^\circ$ to 26.4° is clear indication of possible transformation of ZB phase to W phase. Since the peaks related to W phase are present in all the films, the XRD data have been refined for W lattice [JCDD # 8000006]. The values of electronegativity for Pb (2.33) and Cd (1.69), which are not favourable to form a solid solution [22]. In CdSPb25 film, peaks indicated angular positions at $2\theta = 13.57^\circ$ and 15.9° corresponding to $[\text{Pb}(\text{NH}_2(\text{S})\text{C}(\text{NH}_2)_2)_2](\text{ClO}_2)_2$, i.e., lead perchlorate thiourea, according to standard (JDDC 053-1447). In the alkaline medium of CB, the atom-atom growth of CdS is supposed to proceed by decomposition of adsorbed thiourea-hydroxo-cadmium complex as expressed by [23]



In our opinion, this result indirectly proves the mechanism proposed by Ortega-Borges and Lincot [24]. In this mechanism the rate-determining step is the metastable complex decomposition for which activation energy values are close to those calculated and that can be expected. On the basis of the above CdS0 precipitation mechanism, the high $V_{[\text{Pb}^{2+}]}$ can be assured that is not leading to the CdS0 large cluster, causing instead a non-uniform thin film in CdS:Pb growth. Because the more metastable complex can acquire enough activation energy to decompose and to precipitate, the crystalline CdS0 film is due to high $V_{[\text{Pb}^{2+}]}$. It should be noticed that CdSPb is not only formed, but also Cl^- and ClO_4^- ions are generated in the system; the coproduced ClO_4^- anion is thus oxidized by the reduction. In this $V_{[\text{Pb}^{2+}]}$, a Cl^- ion is oxidized by the NO_3^- in the system affording ClO_4^- , according to:



PbS0 sample diffractogram display peaks located at the following angular positions: $2\theta = 26.00^\circ$, 30.07° , 43.10° , 51.00° , 53.48° . They are related to the (111), (200), (220), (311), (222) reflection planes for the ZB phase of the PbS0 respectively. All the diffraction peaks for PbS0 can be perfectly matched to the reference patterns (JCPDS 05-0592) displaying the ZB crystalline phase.

4. Conclusions

The E_g was estimated by assuming a direct transition and it was found to be slightly increasing with thickness of films and doping. The absorption coefficient was deduced from the transmittance measurements and tailing in low energy side was observed. From the plot of natural logarithm of the ab-

sorption coefficient against the photon energy it was found that the tailing follows Urbach rule. The width of the tail was estimated and found to decrease with thickness of films and doping due to an increase of order. A linear relationship was found between the band gap energy and the width of Urbach tail.

1. M.A. Islam, Yusuf Salaiman, Nowshad Amin, *Chalcogenide Letters* **8** (2011) 65-75.
2. R. Lozada Morales, O. Portillo Moreno, S. A. Tomas, O. Zelaya Angel, *Optical Materials* **35** (2013) 1023-1028.
3. R. Palomino Merino, O. Portillo Moreno, L. A. Chaltel Lima, R. Gutierrez Perez, M. De Icaza Herrera, and V. Castaño, *Nanocrystalline thin films. Journal of Nanomaterials* <http://dx.doi.org/10.1155/2013/507647>
4. S. Mahanty, D. Basak, F. Rueda, M. León, *J. Electron. Materials* **28** (1999) 559-564.
5. V. Bilgin, S. Kose, F. Atay, and I. Akuz, *Mater Chem. Phys.* **94** (2005) 103-308.
6. O. Portillo Moreno *et al.*, *Properties of PbS:Ni²⁺ Nanocrystals in thin films by chemical bath deposition* ISRN Nanotechnology <http://dx.doi.org/10.1155/2013/507647>.
7. Shadia Jamil Ikhmayies, Riyand N. Ahmad-Bitar, *J. of Mater Res. Technol* **2** (2013) 221-227.
8. P.P. Sahay, R.K. Nath, S. Tewari, *Cryst. Res. Technol.* **42** (2007) 275-280.
9. O. Portillo Moreno *et al.*, *J. of Electrochem. Soc.* **153** (2006) 926-930.
10. Sonal Singhal, Amit Kumar Chawla, Hari Om Gupta, Ramesh Chandra, *Nanoscale Res. Lett.* **5** (2010) 323-331.
11. K. Subba Ramaiah, R.D. Pilkington, A.E. Hill, R.D. Tomlinson, A.K. Bhatnagar, *Mat. Chem. and Phys.* **68** (2001) 22-30.
12. A. Abdolazaden Ziabari, F.E. Ghodsi, *J. of Luminescence* **141** (2013) 121-129.
13. M.A. Barote, A.A. Yadav, L.P. Deshmukh, E. U. Masumdar, *J. of Non-Oxide Glasses* **2** (2010) 151-165.
14. Hani Khallaf, Guangyu Chai, Oleg Lupan Lee Chow, S. Park, A. Schulte, *J. Phys. D: Appl. Phys.* **41** (2008) 185304.
15. Hideyuki Kanazawa and Sadao Adachi, *J. Appl. Phys.* **83** (1998) 5997-6001.
16. A. Cortes, H. Gómez, R.E. Marotti, G. Riveros, E.A. Dalchiele, *Solar Energy Materials & Solar Cell.* **82** (2004) 21-34.
17. J. Pantoja Enríquez, X. Mathew, *Solar Energy Mat. & Solar cell.* **76** (2003) 313-322
18. J. Melsheimer, D. Ziegler, *Thin Solid Films.* **129** (1895) 35-37.
19. Koichi Yamaguchi, Tsukasa Yoshida, Takashi Sugiura, Hideki Minourea, *J. Phys. Chem.* **B10** (1998) 9677-9686.
20. J.A. Dávila Pintle *et al.*, *J. of Appl. Phys.* **101** (2007) 013712-1, 013712-5.
21. M. Kamruzzaman, R. Dutta, J. Podder, *Semiconductors* **46** (2012) 957-961.
22. J.A. Lange's *Handbook of Chemistry*, (McGraw-Hill Book Co., Beijing, 1999).
23. M. Froment and D. Lincot, *Phase formation process in the solution at atomic level: Metal chalcogenide semiconductor* *Electrochimica Acta* **40** (1995) 1293-1303.
24. R. Ortega-Borges, D. Lincot, *J. Electrochem. Soc.* **140** (1993) 3464.